Chemical Science

ROYAL SOCIETY OF CHEMISTRY

EDGE ARTICLE

View Article Online
View Journal | View Issue

Cite this: *Chem. Sci.*, 2023, **14**, 3370

All publication charges for this article have been paid for by the Royal Society of Chemistry

Received 13th January 2023
Accepted 26th February 2023

DOI: 10.1039/d3sc00228d

rsc.li/chemical-science

CO_2-switchable emulsions with controllable size and viscosity†

Jianzhong Jiang, * Huaixin Li and Yao Gu

CO_2-responsive emulsions have attracted considerable attention in recent years because of their biocompatibility and easy removal of CO_2. However, most CO_2-responsive emulsions are only used in stabilization and demulsification processes. In this paper, we report CO_2-switchable oil-in-dispersion (OID) emulsions co-stabilized with silica nanoparticles and anionic NCOONa, in which the required concentrations of NCOONa and silica particles were as low as 0.01 mM and 0.0001 wt%, respectively. Besides reversible emulsification/demulsification, the aqueous phase containing the emulsifiers was recycled and reused with the CO_2/N_2 trigger. More importantly, the properties of the emulsions, such as droplet sizes (40–1020 μm) and viscosities (6–2190 Pa s), were intelligently controlled by the CO_2/N_2 trigger, and meanwhile reversible conversion between OID emulsions and Pickering emulsions was achieved. The present method offers a green and sustainable way to regulate the emulsion states, which enables smart control of emulsions and widens their potential applications.

1 Introduction

Stimuli-responsive surfactants are special amphiphilic compounds containing stimuli-responsive groups in their molecular structures,[1] and their surface activities and aggregation behaviours can be changed with environmental stimuli.[2] To date, various triggers for stimuli-responsive surfactants have been reported, including pH,[3,4] CO_2/N_2,[5–9] temperature,[10,11] redox reagents,[12–14] light,[15–17] magnetism,[18–20] and so on. Jessop *et al.* have pioneered a series of CO_2-responsive surfactants and materials,[5,6] in which CO_2 was recognized as one of the inexpensive, green, and biocompatible triggers. Moreover, it is easy to remove CO_2 from product streams without contamination.[21–24] Therefore, considerable effort has been devoted to exploring CO_2-responsive emulsions in recent years.[25–28] However, most of the CO_2-responsive emulsions were based on demulsification/stabilization processes, while the properties of the emulsions (*e.g.* droplet size and viscosity) were rarely regulated with a CO_2 trigger.

Pickering emulsions stabilized with colloid particles have received increasing attention in recent years due to their many applications in foods, cosmetics, and functional materials.[28,29] Compared with conventional emulsions, Pickering emulsions have much higher stabilities due to nearly irreversible adsorption of surface-active particles at the oil–water interface.[30] However, the high stabilities of Pickering emulsions always cause difficulties during demulsification, which might hinder their applications in which temporary stability is needed, such as in emulsion catalysis,[31,32] enzymatic catalysis[33] and emulsion polymerization.[34]

Recently, oil-in-dispersion (OID) emulsions stabilized with similarly charged surfactants and nanoparticles have been reported,[35] in which the surfactants were adsorbed at the oil–water interface and the nanoparticles remained in the aqueous phase. Similar to conventional emulsions, the OID emulsions showed fluidity as good as water, which benefitted applications in oil pipeline transportation and in cutting fluids for which low viscosity was needed.[36] However, OID emulsions are always only temporarily stable (for less than one month), which limits their applicability when long-term stability is required, such as in foods and cosmetics.[37,38] Recently, transformations between OID emulsions and Pickering emulsions have been achieved with pH and redox triggers;[39,40] however, the accumulation of salts during pH changes or redox reactions always affected the stability of the emulsion.

Herein, we report a CO_2/N_2-responsive OID emulsion stabilized with a CO_2-responsive surfactant (11-(*N*,*N*-dimethylamino) sodium undecanoate, NCOONa) aided by a trace amount of silica

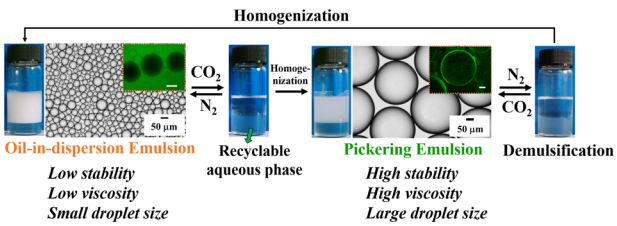

Scheme 1 Schematic diagram of reversible conversion between OID emulsions and Pickering emulsions with the CO_2/N_2 trigger (0.3 mM NCOONa plus 0.1 wt% silica nanoparticles).

The Key Laboratory of Synthetic and Biological Colloids, Ministry of Education, School of Chemical and Material Engineering, Jiangnan University, 1800 Lihu Road, Wuxi, Jiangsu, P.R. China. E-mail: jzjiang@jiangnan.edu.cn

† Electronic supplementary information (ESI) available. See DOI: https://doi.org/10.1039/d3sc00228d

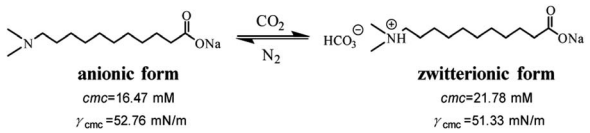

Scheme 2 Chemical structure of anionic NCOONa and its CO_2/N_2 responsiveness.

nanoparticles. Reversible transformation between an OID emulsion and a Pickering emulsion was obtained with a CO_2 trigger. Additionally, the viscosities and droplet sizes of the emulsions were changed with the CO_2 trigger (Scheme 1).

2 Results and discussion

As reported in the literature,[7,8] the tertiary amine group in the NCOONa molecular structure (Scheme 2) responded to the CO_2/N_2 trigger at ambient temperature. Therefore, NCOONa reversibly interconverted between its anionic and zwitterionic (N^+COONa) states at room temperature with the CO_2/N_2 trigger (Scheme 2 and Fig. S1†). However, NCOONa cannot be protonated to the cationic form[41] since the pH of the solution cannot be decreased below 4.4 by bubbling CO_2 (Fig. S2†). The structural transformation of NCOONa was confirmed by the significant chemical shifts of the methylene and methyl groups in the ^{1}H-NMR spectrum after the protonation of the tertiary amines by bubbling CO_2 (Fig. S3†).

The surface activity parameters of the surfactants were listed in Table S1.† NCOONa (pH = 8.35 ± 0.01) showed a much higher cmc (16.47 mM) than other anionic surfactants (*e.g.*, SDS or $C_{11}H_{23}$COONa) because of the weakly polar tertiary amine groups present at the ends of the alkyl chains, which reduced the hydrophobicity of the surfactant. After bubbling CO_2 (pH = 4.54 ± 0.02), the Γ^{∞} of zwitterionic N^+COONa (1.83×10^{-10} mol cm^{-2}) decreased to approximately half of that of NCOONa (3.08×10^{-10} mol cm^{-2}) due to the formation of a second hydrophilic group (aminium bicarbonate) in the molecular structure of N^+COONa, which doubled the cross-sectional area (0.91 nm^2 per molec) of the initial surfactant (NCOONa, 0.54 nm^2 per molec) and increased the cmc (21.78 mM). In contrast to other CO_2-responsive surfactants (*e.g.*, alkyl amidines or alkyl tertiary amines), which were transformed into oil-soluble inactive states by CO_2/N_2 triggers,[8] NCOONa can be converted into a more hydrophilic zwitterionic surfactant (N^+COONa) with less surface activity after bubbling CO_2.

2.1 OID emulsions co-stabilized with NCOONa and silica particles

In contrast to SDS, no stable emulsion can be formed with NCOONa alone below 3 mM due to its strong hydrophilicity (Fig. S4†). After adding 0.1 wt% hydrophilic silica nanoparticles (Fig. S5†), stable emulsions were obtained at low NCOONa concentrations (0.01 mM, 0.00061 cmc) (Fig. 1). The dilution and stained oil phase methods confirmed the O/W morphology (Fig. S6a†). The SEM image of the dried emulsion droplets and the fluorescent micrograph of the emulsion made with labeled silica particles indicated that the silica particles were dispersed in the aqueous phase of the OID emulsions (Fig. 2 and S7a†).[35,42]

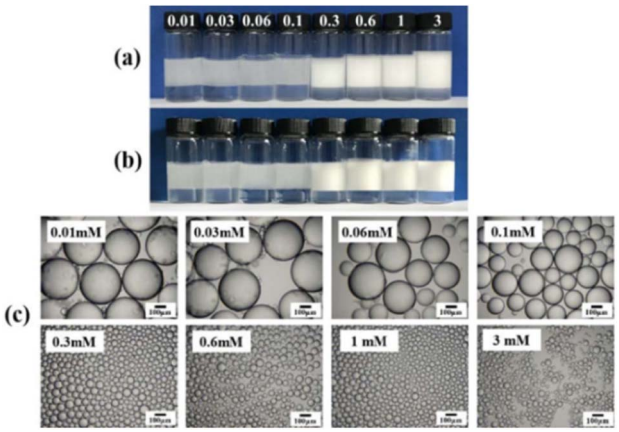

Fig. 1 (a and b) Photographs and (c) micrographs of the OID emulsions prepared with 0.1 wt% silica particles and different concentrations of NCOONa (pH = 8.35). (a) Taken immediately after preparation and (b) and (c) taken 24 h after preparation.

After increasing the NCOONa concentration from 0.01 mM to 0.3 mM, the average droplet diameter of the OID emulsions decreased from 350 μm to 50 μm. However, the droplet diameter did not change with the particle concentration, which is similar as other OID emulsions in the literature.[35,43] The OID emulsions were stable for more than seven days when using 0.0001 wt% silica particles and 0.3 mM NCOONa (Fig. S8†). In addition, the oil–water ratio of the OID emulsions could be freely adjusted from 4 : 6 to 8.5 : 1.5 (stable over 7 days) (Fig. S9†), which exceeded the definition of high internal phase emulsions (HIPEs, 7.4 : 2.6). However, the emulsion was unstable at an oil–water ratio of 9 : 1 because the concentrations of the emulsifiers (NCOONa plus silica particles) were too low to form a thick lamella and prevent coalescence at a high internal oil phase (>90%).[44]

2.2 CO_2 responsiveness of the OID emulsion

The OID emulsions co-stabilized with NCOONa and silica particles showed excellent CO_2/N_2 responsiveness due to the CO_2-responsive tertiary amine group in NCOONa. After bubbling CO_2 for 15 min at room temperature (Fig. 3a), the emulsion was demulsified quickly, and the oil and water phases were separated entirely (Fig. 3b). NCOONa was converted into its zwitterionic form (N^+COONa), which desorbed from the oil–water interface and entered the water phase, resulting in demulsification. Furthermore, the aqueous phase containing the emulsifiers (N^+COONa and silica nanoparticles) could be reused and recycled. As shown in Fig. 3d, a mixture of the separated aqueous phase and a new oil phase yielded a stable OID emulsion after the removal of CO_2 by bubbling with N_2 at room temperature. This reversible cycling of the aqueous phase was carried out at least 10 times with the CO_2/N_2 trigger (Fig. S10†), and the droplet size did not change significantly.

The separated *n*-octane phase showed an interfacial tension similar to that of fresh *n*-octane (50.36 ± 1 mN m^{-1}, Table 1), which confirmed that there was little residual emulsifier left in the oil phase. Similar results were obtained from the ^{1}H NMR

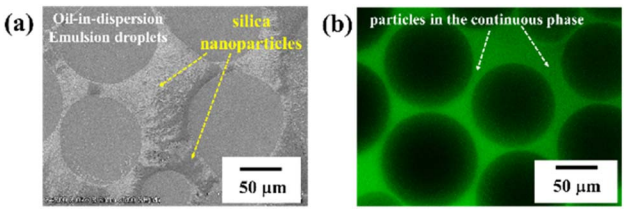

Fig. 2 (a) SEM image of the dried OID emulsion of 0.3 mM NCOONa and 0.1 wt% silica particles (pH = 8.35). (b) Fluorescence micrograph of the OID emulsions using fluorescent-labeled silica particles.

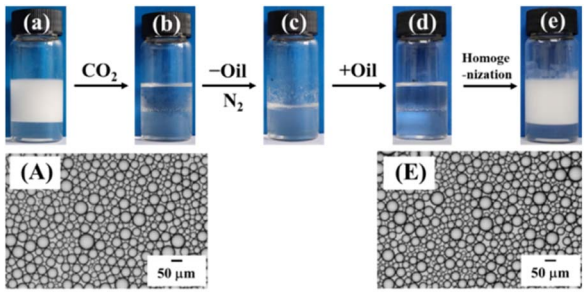

Fig. 3 CO_2/N_2 responsiveness of the OID emulsions co-stabilized with 0.1 wt% silica nanoparticles and 0.3 mM NCOONa with a recyclable aqueous phase. (a) Photograph and (A) micrograph of the initial emulsion (pH = 8.35). (b) Demulsification after bubbling CO_2 (pH = 4.54). (c) The aqueous phase after the removal of the upper oil phase. (d) The mixture of the aqueous phase and new oil after bubbling N_2 (pH = 8.34). (e) Photograph and (E) micrograph of (d) the system after homogenization.

spectrum of the recovered *n*-octane (Fig. S11†). In our previous studies,[9] alkylammonium bicarbonate was deprotonated into an oil-soluble alkyl amine after bubbling N_2, which entered into the oil phase and contaminated the products in the oil phase. Herein, the reuse and recycling of NCOONa from the aqueous phase was obtained with a CO_2 trigger (Fig. 4) without contamination in the oil phase, which has great potential for achieving green and sustainable operations of oil-soluble products in practical applications.

Table 1 The interfacial tension between water and fresh *n*-octane or separated *n*-octane after demulsification

Oil type	Oil–water interfacial tension (mN m^{-1}) ±1.00
Fresh	50.36
First separated	50.39
Second separated	50.31
Third separated	50.41
Fourth separated	50.56
Fifth separated	50.18
Sixth separated	50.63
Seventh separated	50.22
Eighth separated	50.59
Ninth separated	50.00
Tenth separated	50.13

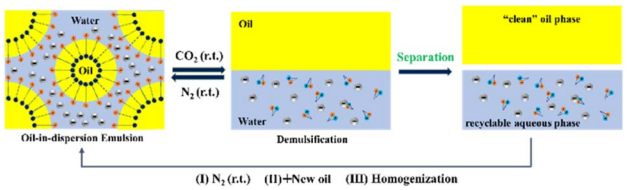

Fig. 4 Mechanism diagram of yielding a recyclable aqueous phase during CO_2/N_2 circulation of OID emulsion.

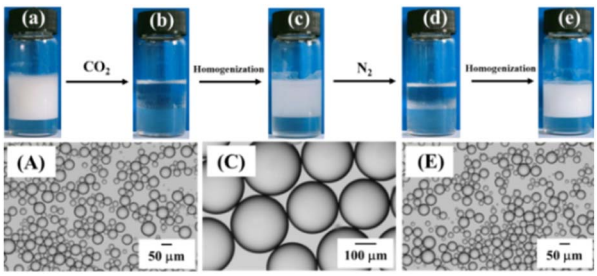

Fig. 5 (a) Photograph and (A) micrograph of the OID emulsions stabilized with 0.1 wt% silica particles and 0.3 mM NCOONa (pH = 8.35). (b) Demulsification after bubbling CO_2 for 15 min at 25 °C (pH = 4.54). (c) Photograph and (C) micrograph of a Pickering emulsion obtained by re-homogenization of the system in (b). (d) Demulsification by bubbling N_2 for 30 min at 25 °C (50 mL min^{-1} and pH = 8.34). (e) Photograph and (E) micrograph of the OID emulsion after re-homogenization of the system in (d).

2.3 Reversible transformation between OID emulsions and Pickering emulsions

In addition to stabilization/demulsification processes and recycling of the emulsifier from the aqueous phase, reversible conversions between OID emulsions and Pickering emulsions could also be realized with the CO_2/N_2 trigger. As shown in Fig. 5c, re-homogenization of the demulsified OID emulsion yielded an O/W Pickering emulsion with higher stability (> one year, Fig. S12†) and a larger droplet size (250 μm).

The staining method confirmed the O/W morphology of the Pickering emulsion (Fig. S6b†). The wrinkled films of the dried droplets were observed in the SEM image (Fig. 6a), which indicated aggregation of the particles at the interface.[45] The fluorescent oil–water interface of the Pickering emulsion with the labeled particles also revealed the location of the silica

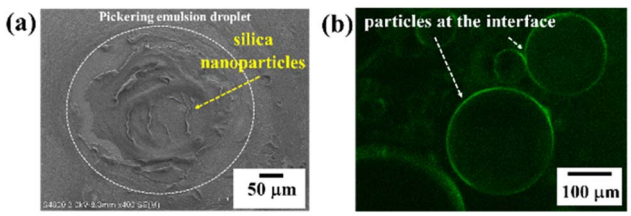

Fig. 6 The Pickering emulsion prepared with 0.3 mM N^+COONa and 0.1 wt% silica particles. (a) SEM photo of dried Pickering emulsion droplets. (b) Fluorescence micrograph of the Pickering emulsions with fluorescent-labeled silica particles.

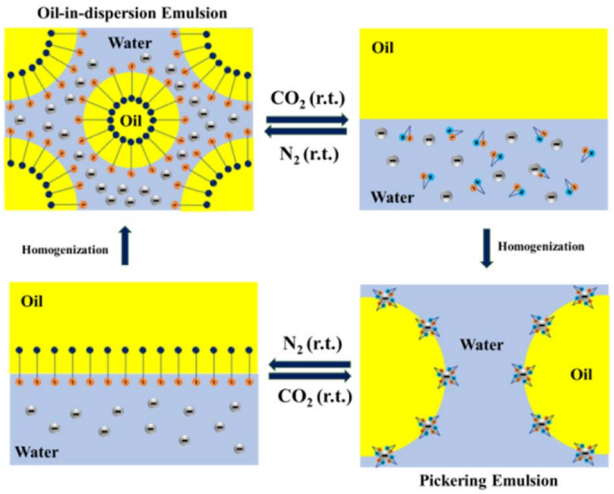

Fig. 7 Mechanism diagram of reversible transition between an OID emulsion and Pickering emulsion through the CO_2/N_2 trigger.

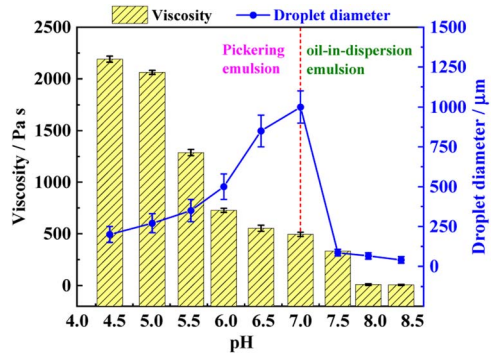

Fig. 8 The droplet size and viscosity of the emulsions stabilized with 0.3 mM NCOONa and 0.1 wt% silica nanoparticles at different pH (4.54–8.35) by bubbling CO_2 (25 mL min^{-1}).

particles at the interface (Fig. 6b). Due to the adsorption of the silica particles at the interface, the Pickering emulsion of N^+COONa and silica particles showed much higher stability and viscosity than the OID emulsions (Fig. 7).

The Pickering emulsions also exhibited excellent CO_2 responsiveness, and they were completely demulsified after the removal of CO_2 (Fig. 5d). After bubbling N_2, N^+COONa was deprotonated to give its anionic form (NCOONa), and it desorbed from the surfaces of silica particles, resulting in demulsification. Furthermore, the OID emulsion was recovered after re-homogenization of the demulsified system, as shown in Fig. 5d.

Although interconversions between the OID emulsions and Pickering emulsions were obtained with the pH and redox reaction triggers,[39,40] the accumulated salts during the switching cycles affected the stabilities and droplet sizes of the emulsions, which limited the number of cycles. For example, the OID emulsions became unstable after 5 cycles with the redox reaction triggers. Interestingly, this conversion between the OID emulsions and the Pickering emulsions was switched at least 20 times with the CO_2 trigger (Fig. S13 and S14†). Since no salt accumulation occurred during the CO_2 switching cycles,[8] reversible transformations between the two emulsion types could be achievable.

Table 2 The pH value, droplet size, and viscosity of the emulsions (0.3 mM NCOONa plus 0.1 wt% silica particles) after bubbling CO_2 for different times (25 mL min^{-1})

Bubbling time/min	pH (±0.01)	Viscosity[a] (±0.02)/Pa s	Average droplet diameter/μm
0	8.35	6.38	40
0.10	7.91	10.20	65
0.15	7.50	329.71	85
0.25	7.00	493.48	1020
0.35	6.47	553.03	848
0.45	5.97	727.20	515
0.75	5.53	1286.97	349
3.20	5.01	2062.30	273
15.00	4.54	2190.86	212

[a] Shear rate = 0.01 s^{-1}.

More importantly, the droplet sizes and viscosities of the emulsions were precisely controlled with the CO_2 trigger (Fig. 8). The pH of NCOONa solution (0.3 mM) gradually changed from 8.3 to 4.6 after bubbling CO_2 (25 mL min^{-1}, Fig. S2† and Table 2). For example, the system's pH (0.3 mM NCOONa) decreased to 7 and then to 4.6 after bubbling with CO_2 for 0.25 min and 15 min, respectively. The viscosity of the emulsion increased from 6.38 Pa s (pH = 8.3 and shear rate = 0.01 s^{-1}) to 2200 Pa s (pH = 4.6 and shear rate = 0.01 s^{-1}) (Fig. 8 and Table 2), while the droplet sizes of the emulsion gradually increased from 40 μm (pH = 8.3) to 1020 μm (pH = 7) and then decreased to 212 μm (pH = 4.5) (Fig. 8 and S15†). This occurred because anionic NCOONa gradually converted into zwitterionic N^+COONa after bubbling CO_2, and the fluid-like OID emulsions were converted into viscous Pickering emulsions when the pH was lower than 7.0 (Fig. 8). As the pH further decreased by bubbling CO_2, the efficiency for adsorption of N^+COONa on the surfaces of the silica particles increased with increasing N^+COONa concentration, which resulted in further increases in the viscosity of the Pickering emulsions and a decrease in the droplet size.

2.4 Mechanism analysis

The surface tension of anionic NCOONa decreased slightly after adding similarly charged silica particles, indicating there was no adsorption of the surfactant on the particle surfaces (Fig. S16a†). After NCOONa concentration was increased from 0.01 mM to 10 mM, the zeta potential of the silica particles changed from −41.7 mV to −32.8 mV (Fig. 9a), indicating that NCOONa served as an electrolyte to compress the electric double layer of the silica particles.[46] The contact angle of *n*-octane on the glass plate using the inverted sessile method (Fig. S17 and S18†) also indicated that there was no adsorption of anionic NCOONa on the silica particles, since the contact angles were almost the same (24.5° ± 2°) with different NCOONa

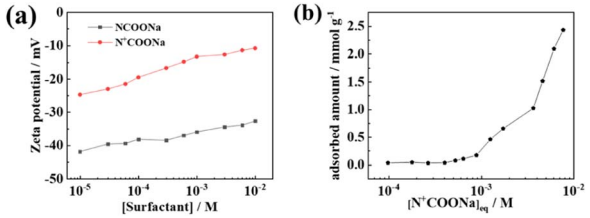

Fig. 9 (a) Zeta potential of silica particles dispersed in NCOONa/N^+COONa solutions with different concentrations; (b) the curve of the adsorbed amount of N^+COONa on the particles as a function of the equilibrium surfactant concentration.

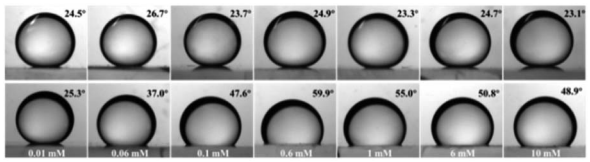

Fig. 10 Contact angles of *n*-octane drops (inverted) captured by a glass slide immersed in NCOONa (upper) and N^+COONa (lower) aqueous solutions at 25 °C. The surfactant concentration (mM^{-1}) from left to right: 0.01, 0.06, 0.1, 0.6, 1, 6, 10.

concentrations (Fig. 10). Therefore, the anionic NCOONa was adsorbed at the oil–water interfaces in the OID emulsions to reduce the interfacial tension and endow the droplets with negative charges, while the silica particles were dispersed in the aqueous phase. The distance between two droplets of the emulsions in the absence of silica particles was 35 nm (0.3 mM NCOONa), which was double the Debye length ($\kappa^{-1} = 17.6$ nm). However, the distance could increase to 270 nm ($4\kappa^{-1}$ + particle size (~200 nm, Fig. S5†)) if one particle was present between the two droplets (Fig. S19†). Therefore, the van der Waals attraction between the droplets decreased after the increase of the distance between the oil droplets. Furthermore, since there was more than one particle surrounding the droplets, the van der Waals attractions could be further reduced. The particle–droplet and particle–particle electric double layer repulsions together with the reduced van der Waals attractions prevented the droplets from undergoing flocculation or coalescence.[35,46,47]

After bubbling CO_2, anionic NCOONa gradually converted into zwitterionic N^+COONa, which decreased the surfactant's charge density and weakened the electrical double layer repulsions of the OID emulsions, and led to demulsification. Compared with NCOONa, zwitterionic N^+COONa has a higher polarity, stronger hydrophilicity, and lower surface activity due to its two hydrophilic head groups. Therefore, N^+COONa desorbed from the oil–water interface and entered the aqueous phase. Furthermore, the hydrophilic silica particles also remained in the aqueous phase after demulsification. The "clean" oil phase was separated after demulsification without further purification (Fig. 3 and Table 1). Since NCOONa could be recovered by removal of CO_2, the OID emulsion was reformed with the fresh oil phase and the aqueous phase containing the emulsifiers (N^+COONa plus silica particles) after bubbling N_2 (Fig. 3c). Therefore, the emulsifiers could be reused and recycled from the aqueous phase without contamination in the oil phase.

It was reported that the positively charged amino group was stronger than the anionic carboxylate group in the surfactant structure.[42] Therefore, zwitterionic N^+COONa exhibited the characteristics of a weak cationic surfactant because the positive charges were partially neutralized by the carboxylate groups. The zeta potential of the silica particles in pure water decreased to −25 mV after bubbling CO_2.[48,49] A slight change in the zeta potential (from −24.9 mV to −10.7 mV) of the silica particles was observed after increasing the surfactant (N^+COONa) concentration from 0.01 mM to 10 mM (Fig. 9a). Therefore, N^+COONa adsorbed on the surfaces of the silica particles as a cationic surfactant and the electrostatic attractions operated during the homogenization process. Contact angle measurements also indicated the adsorption of the zwitterionic surfactant (N^+COONa) on the surface of silica particles with increasing hydrophobicity (Fig. 10). Furthermore, the contact angle increased from 25.3° to 59.9° after zwitterionic surfactant (N^+COONa) concentration was increased from 0.01 mM to 0.6 mM, indicating the formation of a surfactant monolayer on the particle surfaces.[50–52] However, the contact angle decreased after N^+COONa concentration was increased further, possibly due to hydrophobic interactions between the carbon chains, and this resulted in the formation of bilayers or semi-micelles on the particle surfaces.[53] Moreover, the surface tension of the zwitterionic form (N^+COONa) increased after adding a trace amount of silica particles due to the adsorption of the surfactant on the particles (Fig. S16b†). The amount of N^+COONa adsorbed on the silica particles was 0.031 mmol g^{-1} (Fig. 9b) at an equilibrium concentration of 0.27 mM, and the molecular cross-sectional area of the N^+COONa molecule at the interface was 9.54 nm^2, which was much larger than that of N^+COONa molecules adsorbed at the saturation level at the air–water interface (0.91 nm^2 per molec). At this time, N^+COONa formed a loose monolayer adsorbed on the silica particles.[53,54]

After bubbling N_2, N^+COONa was converted to its anionic form (NCOONa), and the positive charges on the surfactant molecules were eliminated, which resulted in the desorption of the surfactant from the silica particles. Therefore, the Pickering emulsions were demulsified completely by the N_2 trigger. Moreover, the OID emulsions were recovered after re-homogenization of the demulsified system containing silica particles and NCOONa. Therefore, reversible transformations between the Pickering emulsions and OID emulsions occurred (Fig. 7), and the stability as well as the viscosity and droplet size were efficiently controlled with the CO_2/N_2 trigger (Fig. 8).

3 Conclusions

In summary, we report a switchable surfactant (NCOONa) that can be converted reversibly between anionic and zwitterionic states with the CO_2/N_2 trigger. CO_2-responsive OID emulsions, including HIPEs, were co-stabilized with NCOONa and silica particles at low concentrations (0.01 mM and 0.0001 wt%,

respectively). Since anionic NCOONa was converted into the more hydrophilic N^+COONa, stabilization and destabilization of the emulsion were achieved with the CO_2/N_2 trigger, and the emulsifiers (surfactant plus the particles) were also recycled from the aqueous phase with no residual surfactant left in the oil phase. Furthermore, reversible interconversions between OID emulsions and Pickering emulsions were realized with the CO_2/N_2 trigger, and the droplet sizes (40–1020 μm) and viscosities (6–2190 Pa s) of the emulsions could be changed precisely. This strategy provides smart emulsions with adjustable properties to meet different application requirements, such as those of two-phase catalysis, emulsion polymerization, cutting fluids, and oilfield exploitation.

Data availability

Experimental and the emulsion data (in pdf) have been included.

Author contributions

J. J. performed the conceptualization, methodology, project administration, supervision, funding acquisition, and writing and reviewing. H. L. performed the investigation, data curation, and writing the original draft. Y. G. performed the data curation.

Conflicts of interest

There are no conflicts to declare.

Acknowledgements

This work was supported by the National Natural Science Foundation of China (No. 21872064). We also thank the Central Laboratory, School of Chemical and Material Engineering, Jiangnan University for help in using instruments and various measurements.

Notes and references

1 P. Brown, C. P. Butts and J. Eastoe, *Soft Matter*, 2013, **9**, 2365–2374.
2 Z. Jiang, X. Li, G. Yang, L. Cheng, B. Cai, Y. Yang and J. Dong, *Langmuir*, 2012, **28**, 7174–7181.
3 J. Tan, J. Wang, L. Wang, J. Xu and D. Sun, *J. Colloid Interface Sci.*, 2011, **359**, 155–162.
4 L. Liu, X. Pu, Y. Zhou, J. Zhou, D. Luo and Z. Ren, *Colloids Surf., A*, 2020, **586**, 124246.
5 Y. Liu, P. G. Jessop, M. Cunningham, C. A. Eckert and C. L. Liotta, *Science*, 2006, **313**, 958–960.
6 A. Darabi, P. G. Jessop and M. F. Cunningham, *Chem. Soc. Rev.*, 2016, **45**, 4391–4436.
7 X. Su, P. G. Jessop and M. F. Cunningham, *Macromolecules*, 2012, **45**, 666–670.
8 P. G. Jessop and M. F. Cunningham, *CO_2-Switchable Materials: Solvents, Surfactants, Solutes and Solids*, Royal Society of Chemistry, 2020.
9 S. Yu, D. Zhang, J. Z. Jiang, Z. Cui, W. Xia, B. P. Binks and H. Yang, *Green Chem.*, 2019, **21**, 4062–4068.
10 M. Wang, K. Zhang, W. Wu, J. Chen and P. Zhang, *Colloids Surf., A*, 2011, **385**, 126–133.
11 Y. Zhu, T. Fu, K. Liu, Q. Ling, X. Pei, J. Jiang, Z. Cui and B. P. Binks, *Langmuir*, 2017, **33**, 5724–5733.
12 Y. Takahashi, N. Koizumi and Y. Kondo, *Langmuir*, 2016, **32**, 7556–7563.
13 C. E. Banks, T. J. Davies, R. G. Evans, G. Hignett, A. J. Wain, N. S. Lawrence, J. D. Wadhawan, F. Marken and R. G. Compton, *Phys. Chem. Chem. Phys.*, 2003, **5**, 4053–4069.
14 H. Sun, M. Li, L. Li, T. Liu, Y. Luo, T. P. Russell and S. Shi, *J. Am. Chem. Soc.*, 2021, **143**, 3719–3722.
15 J. Jiang, Y. Ma, Z. Cui and B. P. Binks, *Langmuir*, 2016, **32**, 8668–8675.
16 C. Xie, S. Meng, L. Xue, R. Bai, X. Yang, Y. Wang, Z. Qiu, B. P. Binks, T. Guo and T. Meng, *Langmuir*, 2017, **33**, 14139–14148.
17 H. Sun, L. Li, T. P. Russell and S. Shi, *J. Am. Chem. Soc.*, 2020, **142**, 8591–8595.
18 P. Brown, T. A. Hatton and J. Eastoe, *Curr. Opin. Colloid Interface Sci.*, 2015, **20**, 140–150.
19 O. Owoseni, E. Nyankson, Y. Zhang, D. J. Adams, J. He, L. Spinu, G. L. McPherson, A. Bose, R. B. Gupta and V. T. John, *J. Colloid Interface Sci.*, 2016, **463**, 288–298.
20 B. Yao, X. Zhang, F. Li, C. Li and Y. Dong, *ACS Appl. Nano Mater.*, 2020, **3**, 10360–10368.
21 Z. Wang, G. Ren, J. Yang, Z. Xu and D. Sun, *J. Colloid Interface Sci.*, 2019, **536**, 381–388.
22 M. F. Cunningham and P. G. Jessop, *Macromolecules*, 2019, **52**, 6801–6816.
23 A. Chen, J. Chen, D. Wang, J. Xu and H. Zeng, *J. Colloid Interface Sci.*, 2020, **571**, 134–141.
24 Q. Zhang, L. Lei and S. Zhu, *ACS Macro Lett.*, 2017, **6**, 515–522.
25 Y. Shi, D. Xiong, Z. Li, H. Wang, J. Qiu, H. Zhang and J. Wang, *ACS Appl. Mater. Interfaces*, 2021, **12**, 53385–53393.
26 Z. Sun, Q. Zhao, R. Haag and C. Wu, *Angew. Chem., Int. Ed.*, 2021, **60**, 8410–8414.
27 L. Liu, M. Zhang, Z. Lu, Z. Jin, Y. Lu, D. Sun and Z. Xu, *J. Colloid Interface Sci.*, 2022, **627**, 661–670.
28 H. Jin, P. G. Jessop and M. F. Cunningham, *Colloid Polym. Sci.*, 2022, **300**, 375–385.
29 J. Texter, *Colloid Polym. Sci.*, 2022, **300**, 587–592.
30 B. P. Binks, *Curr. Opin. Colloid Interface Sci.*, 2002, **7**, 21–41.
31 S. Wiese, A. C. Spiess and W. Richtering, *Angew. Chem., Int. Ed.*, 2013, **52**, 576–579.
32 H. Zou, H. Shi, S. Hao, Y. Hao, J. Yang, X. Tian and H. Yang, *J. Am. Chem. Soc.*, 2023, **145**, 2511–2522.
33 K. Li, H. Zou, R. Ettelaie, J. Zhang and H. Yang, *Angew. Chem., Int. Ed.*, 2023, e202300794.
34 Z. Zhang, M. Cheng, M. San Gabriel, A. A. Teixeira Neto, J. d. S. Bernardes, R. Berry and K. C. Tam, *J. Colloid Interface Sci.*, 2019, **555**, 489–497.

35 M. Xu, J. Jiang, X. Pei, B. Song, Z. Cui and B. P. Binks, *Angew. Chem., Int. Ed.*, 2018, **57**, 7738–7742.
36 K. Mohammadzadeh, S. H. Hashemabadi and S. Akbari, *J. Nat. Gas Sci. Eng.*, 2016, **29**, 355–364.
37 I. Tavernier, W. Wijaya, P. Van der Meeren, K. Dewettinck and A. R. Patel, *Trends Food Sci. Technol.*, 2016, **50**, 159–174.
38 D. Venkataramani, A. Tsulaia and S. Amin, *Adv. Colloid Interface Sci.*, 2020, **283**, 102234.
39 J. Jiang, S. Yu, W. Zhang, H. Zhang, Z. Cui, W. Xia and B. P. Binks, *Angew. Chem., Int. Ed.*, 2021, **60**, 11793–11798.
40 Y. Liu, H. Zhang, W. Zhang, B. P. Binks, Z. Cui and J. Z. Jiang, *Angew. Chem., Int. Ed.*, 2023, **62**, e202210050.
41 I. B. Ustunol, N. I. Gonzalez-Pech and V. H. Grassian, *J. Colloid Interface Sci.*, 2019, **554**, 362–375.
42 M. Xu, W. Zhang, J. Z. Jiang, X. Pei, H. Zhu, Z. Cui and B. P. Binks, *Langmuir*, 2020, **36**, 15543–15551.
43 M. Lv, Q. Meng, W. Si, M. Hao, R. Han, Y. Lai, J. Jiang and Z. Cui, *Colloids Surf., A*, 2022, **641**, 128541.
44 I. Akartuna, A. R. Studart, E. Tervoort and L. J. Gauckler, *Adv. Mater.*, 2008, **20**, 4714–4718.
45 B. P. Binks and J. A. Rodrigues, *Angew. Chem., Int. Ed.*, 2007, **46**, 5389–5392.
46 H. Zhang, M. Lv, J. Jiang, Z. Cui, W. Xia and B. P. Binks, *Chem. Sci.*, 2021, **12**, 11845–11850.
47 H. Zhang, J. Wu, J. Jiang, Z. Cui and W. Xia, *Langmuir*, 2020, **36**, 14589–14596.
48 J. Coreno, A. Martinez, A. Bolarin and F. Sanchez, *J. Biomed. Mater. Res.*, 2001, **57**, 119–125.
49 S. Park and H. B. Lee, *Colloid Polym. Sci.*, 2012, **290**, 445–455.
50 R. O. Skoeld and M. A. R. Tunius, *Langmuir*, 1994, **10**, 211–217.
51 S. Yu, H. Zhang, J. Jiang, Z. Cui, W. Xia and B. P. Binks, *Green Chem.*, 2020, **22**, 5470–5475.
52 L. Ma, M. Zhu and T. Liu, *Colloids Surf., A*, 2022, **644**, 128877.
53 B. Chen, J. Liu, S. Shan and W. Yang, *Colloids Surf., A*, 2021, **618**, 126500.
54 E. Dickinson, R. Ettelaie, T. Kostakis and B. S. Murray, *Langmuir*, 2004, **20**, 8517–8525.